

# A reanalysis of the X-ray luminosities of clusters of galaxies in the EMSS sample with $0.3 < z < 0.6$ .

S.C. Ellis<sup>\*</sup> and L.R. Jones

*School of Physics and Astronomy, University of Birmingham, Birmingham, B15 2TT, UK.*

Accepted .....; Received .....; in original form .....

## ABSTRACT

The X-ray luminosities of the *Einstein* Extended Medium Sensitivity Survey (EMSS) clusters of galaxies with redshifts  $0.3 < z < 0.6$  are remeasured using *ROSAT* PSPC data. It is found that the new luminosities are on average  $1.18 \pm 0.08$  times higher than previously measured but that this ratio depends strongly on the X-ray core radii we measure. For the clusters with small core radii, in general we confirm the EMSS luminosities, but for clusters with core radii  $> 250$  kpc (the constant value assumed in the EMSS), the new luminosities are  $2.2 \pm 0.15$  times the previous measurements. The X-ray luminosity function (XLF) at  $0.3 < z < 0.6$  is recalculated and is found to be consistent with the local XLF. The constraints on the updated properties of the  $0.3 < z < 0.6$  EMSS sample, including a comparison with the number of clusters predicted from local XLFs, indicate that the space density of luminous, massive clusters has either not evolved or has increased by a small factor  $\sim 2$  since  $z = 0.4$ . The implications of this result are discussed in terms of constraints on the cosmological parameter  $\Omega_0$ .

**Key words:** galaxies:clusters:general — X-rays:galaxies — cosmology:observations

## 1 INTRODUCTION.

The formation and growth of structure in the Universe depends upon certain fundamental cosmological parameters which govern the environment in which the structures form. Clusters of galaxies, as the largest virialised objects in the Universe, offer a unique insight into the formation of structure and hence into the parameters governing their evolution.

The X-ray properties of clusters offer a useful way of probing this evolution. The X-ray emission is due mainly to bremsstrahlung radiation from the hot intra-cluster gas (which is the dominant component of baryonic matter in clusters) and therefore the X-ray luminosity ( $L_X$ ) is expected to be positively correlated to the system mass. A measurement of the evolution of  $L_X$  is therefore a natural choice for the study of the evolution of clusters of galaxies.

Several surveys have been made in the past which measure the evolution of the X-ray luminosity function (XLF) with differing results. Notably the *Einstein* Extended Medium Sensitivity Survey (EMSS) of Henry et al. (1992) and Gioia et al. (1990) finds moderate negative evolution of the number density of high redshift clusters ( $z > 0.3$ ) of high

$L_X > 5 \times 10^{44}$  ergs  $s^{-1}$ , i.e. there are more high luminosity clusters in the present than there were in the past, but no evolution of moderate luminosity clusters. This agrees well with simple hierarchical formation theories in which the most massive clusters will have formed most recently. More recent surveys, (Rosati et al. 2000; Burke et al. 1997; Vikhlinin et al. 1998a; Jones et al. 1998; Nichol et al. 1999) find no evidence for evolution in the XLF at low to moderate luminosities at  $z < 0.9$ . At high luminosities there remains some ambiguity, probably due to the low numbers of high luminosity clusters in the surveys. There are three surveys, in addition to the EMSS, reporting statistically significant evolution at high luminosities. Vikhlinin et al. (1998a), Rosati et al. (2000) and Gioia et al. (2001) all find moderate (typically a factor  $\sim 3$  in the space density) negative evolution of high luminosity clusters at  $z > 0.3$  (or  $z > 0.5$  in the case of Rosati et al. 2000). Nichol et al. (1999) also find significant evolution but in a non-independent sample based partly on the Vikhlinin et al. (1998a) survey. Contrarily, in the survey of Jones et al. (2000) and Ebeling et al. (2001) no evidence for significant evolution is found at  $z < 0.9$ .

Because any evolution of the XLF would be most apparent at high luminosities (since more massive clusters evolve more quickly than less massive clusters in a bottom-up formation scenario), and because evolution in this most critical

<sup>\*</sup> E-mail: sce@star.sr.bham.ac.uk

part of the XLF is still an area of controversy, it is thus desirable to extend observations of the evolution of the XLF to high luminosity clusters at high redshift. The EMSS remains one of the only samples which contains a reasonable number of high luminosity, massive clusters at high redshift and therefore it is the sample most suited to constraining cluster evolution at high  $L_X$ .

It has been suggested (Jones et al. 1998) that the evolution of the XLF found for high redshift clusters in the EMSS may be partly an artefact due to an incorrect conversion from detected flux to total flux. Furthermore it is suggested that a systematic increase in the fluxes of the EMSS  $z > 0.3$  clusters by a factor of  $\approx 1.25$  would account for the observed difference in the EMSS and *ROSAT*  $\log N - \log S$  relations. An explanation for such a difference is offered by Henry (2000) where it is pointed out that the inclusion of the effect of the *Einstein* point spread function (psf) was omitted when correcting from detected flux to total flux in the original EMSS and that the inclusion of such an effect would increase the total fluxes of  $z > 0.3$  clusters by a mean factor of 1.373. However, it is also pointed out by Henry (2000) that the inclusion of other effects, viz. integrating the cluster emission out only as far as the virial radius (as opposed to infinity as in Henry et al. 1992) and using a slightly different value for the mean King profile surface brightness slope,  $\beta$ , would almost cancel out the correction due to including the psf and thus the original EMSS formulation was fortuitously correct.

The corrections made in converting from detected flux to total flux in the EMSS were large. The original EMSS sample of X-ray clusters were detected using a  $2.4' \times 2.4'$  cell, and the flux falling outside this cell was corrected for assuming a King profile with  $\beta = \frac{2}{3}$  and a core radius of  $r_c = 250$  kpc. The average conversion factor from total flux to detected flux is 1.8 for clusters at  $z > 0.3$  in the EMSS survey, and this factor is very sensitive to the assumed core radius. This correction was never claimed to be applicable to individual clusters by Henry et al. (1992) but rather was used as a mean correction for the sample. There is some evidence that the core radius assumed in deriving the correction is a good average (Vikhlinin et al. 1998a, Table 1 of this paper) although Fig 3. shows that for individual clusters the measured core radius can have a significant effect on the derived luminosity.

Therefore it is possible that the negative evolution seen in the EMSS may not be representative of cluster evolution, and a reanalysis of the luminosities of EMSS clusters is necessary to determine more accurately the evolution of the XLF.

Nichol et al. (1997) have reanalyzed the EMSS sample using *ROSAT* Position Sensitive Proportional Counter (PSPC) data and find that there is evolution of the XLF, albeit at a lower rate than originally found. We feel, however, that a further reanalysis is justified for the reasons given in §2.1.

A reanalysis of the EMSS is also important because the sample has been used to derive X-ray temperature functions (XTFs), which are used to derive accurate values for  $\Omega_0$ . Although the temperatures are independent of the fluxes and core radii, which are remeasured in this paper, the volume surveyed is not. Therefore in order to compute the XTF ac-

curately it is necessary to have reliable measurements of the cluster fluxes.

In this paper we use a simple aperture photometry method to reanalyze the fluxes of the EMSS sample for clusters with  $z > 0.3$  using *ROSAT* PSPC data. We use a large (3 Mpc radius) aperture so that the total fluxes are almost independent of the model surface surface brightness profile. The total fluxes are calculated firstly with the same King profile used in Henry et al. (1992) for a direct comparison with the original *EINSTEIN* data. The core radii of the clusters are then measured from surface brightness fitting and the total fluxes are recalculated using the appropriately corrected King profiles. The XLF is then computed using the new data and compared to the original XLF of Henry et al. (1992). It is assumed that  $H_0 = 50 \text{ km s}^{-1} \text{ Mpc}^{-1}$  and  $q_0 = 0.5$  throughout.

## 2 DATA AND ANALYSIS.

Of the EMSS clusters listed in table 1 of Gioia & Luppino (1994) (which contains redshifts and luminosities of the EMSS clusters) 17 are at  $0.3 < z < 0.6$  and have been observed by *ROSAT*. Of these, 11 have been observed with the PSPC. Note that MS1333.3+1725 has now been identified as a star (Luppino et al. 1999, Molikawa et al. 1999), MS1209.0+3917 as a BL Lac (Rector et al. 1998) and MS1610.4+6616 as (a point source at the position of) a star (Stocke et al. 1999). There also exists a new redshift measurement for MS1241.5+1710 of  $z = 0.549$  (Henry 2000).

### 2.1 Comparisons with the methodology of Nichol et al. (1997).

Although Nichol et al. (1997) have reanalyzed the EMSS sample using *ROSAT* PSPC data we feel that a further reanalysis is necessary. This is because we feel that further improvements can be made to the reanalysis.

Our reanalysis differs from that of Nichol et al. (1997) in three important aspects. Firstly, our samples of clusters at  $z > 0.3$  are different. We adopted the methodology of using the original sample of Henry et al. (1992) as closely as possible but supplemented with newer measurements and identifications wherever appropriate. Accordingly we have used the revised sample of Gioia & Luppino (1994) throughout, except where recent measurements have shown certain objects (viz. MS1333.3+1725, MS1209.0+3917, MS1610.4+6616; see §2) not to be clusters, and we have used new redshift measurements where appropriate. The methodology of Nichol et al. (1997) is somewhat different in that a measurement of the extent of the X-ray emission of each cluster is made to decide whether the object is a cluster or not. Sources which are unresolved in *ROSAT* PSPC data are flagged as uncertain. Some of these sources were then examined in the HRI to check their extent, and for those clusters for which there were no high-quality HRI data Monte Carlo simulations were performed to assess the probability that such compact sources would be observed by the PSPC. Two clusters (at  $z > 0.3$ ) were excluded by Nichol et al. (1997) following this method, and two more were not excluded but were classified as ambiguous. This method of identifying clusters is not satisfactory since MS1208.7+3928,

which was excluded, has been found to be a cluster (Stoeckle et al. 1999); it is also included in the survey of Luppino et al. (1999) and is found independently in the survey of Vikhlinin et al. (1998b). Also two clusters (MS1333.3+1725 and MS1610.4+6616, see §2) which are included by Nichol et al. (1997) have since been found not to be clusters. The two clusters (MS2137.3-2353 and MS1512.4+3647) which were classed as ambiguous in Nichol et al. (1997) are also found to be clusters in HRI observations by Molikawa et al. (1999), which adds further doubt to the robustness of the classification scheme of Nichol et al. (1997).

The second way in which our reanalysis differs with that of Nichol et al. (1997) is in the data reduction method. We have used a spectral cube when performing our background subtraction. This allows the photon vignetting to be calculated more accurately as a function of energy than when using an image in a single passband, as in Nichol et al. (1997), when a mean photon energy must be assumed.

Finally, the third way in which our reanalysis is different to that of Nichol et al. (1997) is in the data analysis. Nichol et al. (1997) measure count rates within a fixed metric aperture that is calculated (as a function of redshift and PSF) to encompass 85 % of the total flux. However this calculation is made assuming a King profile of  $\beta = \frac{2}{3}$  and a core radius of  $r_c = 250$  kpc. We improve upon this by measuring the core radius of each cluster and correcting from detected flux to total flux using the King profile with the measured core radius (see §2.2). The count rates were converted to fluxes assuming a 6 keV Raymond-Smith spectrum in Nichol et al. (1997), whereas we had the advantage of being able to use measured temperatures (for all but one cluster) from ASCA measurements.

## 2.2 Flux measurement.

For each cluster with a PSPC observation the data were reduced in the following way. The raw data were downloaded from the LEDAS ROSPUB archive. The data were first cleaned for bad times and a corrected exposure time was obtained. A spectral cube was sorted, of  $384 \times 384$  spatial bins and 10 energy bins, and a background cube was associated with it. Cubes were used as this makes correcting for photon vignetting more accurate than if images were used when a mean photon energy would have to be assumed. The background was measured in an annulus from  $0.15^\circ - 0.25^\circ$  to avoid the original target of the pointing and the shadows of the window support structure. The cluster was masked out of this background annulus if it were coincident with it. Point sources within the background annulus were removed. The point sources were found using the *ASTERIX PSS* routine (Allan & Vallance 1995) which employs a maximum likelihood search based on the Cash (1979) statistic. The point source searching procedure was iterated until no more significant point sources were found. A final check of the background was made by eye. Any obvious contaminations were removed and the procedure was re-run. The expected particle background was calculated using the method of Snowden et al. (1992). The measured value of the background was then extrapolated over the field as a function of energy, taking into account the unvignetted particle background, and subtracted from the source. The background-

subtracted cube was then corrected for energy-dependent vignetting. The exposure was corrected for dead time.

From the background-subtracted cube the number of counts within an aperture of 3Mpc in radius was extracted (this corresponds to  $9.09'$  at  $z = 0.3$  and  $6.57'$  at  $z = 0.6$ ). Point sources within the aperture found by inspection of raw and smoothed images, were masked out (except in the cluster cores, where the high surface brightness cluster emission may have masked faint point sources). An aperture of 3 Mpc was chosen as the correction to total flux is small and it is much larger than the PSPC psf even at an off-axis angle of  $30'$ . The average error on the count rate was  $\sim 6\%$  based on counting statistics.

The counts within the aperture were corrected assuming a King profile of  $\beta = \frac{2}{3}$  and initially a core radius of  $r_c = 250$  kpc, to obtain the total number of counts. The correction factor for such a profile is 1.09. This correction is based on integrating the emission out to infinity. Whilst it may be more physically accurate to integrate out only as far as the virial radius (Henry 2000), our aim is to compare our *ROSAT* luminosities with the previous measurements of Gioia & Luppino (1994) and Nichol et al. (1997), and to the local XLF of Ebeling et al. (1997), who all integrated to infinity. Henry (2000) notes that because of other effects in the EMSS, although the published EMSS luminosities were integrated to infinite radius, on average they agree with luminosities integrated only to the virial radius, and thus may be correct. We wish to investigate in detail these, and other, effects, in the EMSS luminosities. In order to do this, and to better understand differences with previous work, we will initially follow the method of previous investigations and integrate to infinite radius, but then discuss the effects of integrating only to the virial radius.

To convert from count rates to fluxes a Raymond & Smith (1977) spectral model was assumed. A model spectrum was constructed for each cluster and wherever possible the model parameters were taken from the literature. For the cluster MS0418.3-3844 no measured temperature exists and therefore  $T_X$  was assumed to be 6 keV and for all clusters except MS0451.5-0305 the metallicity is assumed to be  $0.3 \times$  solar. The hydrogen column densities were taken from Dickey & Lockman (1990). Absorbed and unabsorbed fluxes and luminosities were measured in the appropriate energy bands. The model takes into account K-corrections when calculating luminosities.

Exceptions to the method described above were made in the cases of MS0353.6-3642 and MS0418.3-3844. Both these clusters fell very close to the shadow of the window support structure in the PSPC image, and consequently extracting a count rate over a 3 Mpc radius would not yield accurate results. For these clusters radial profiles were taken to estimate the radius at which the surface brightness fell to the background level and the counts within that radius were measured. These radii were  $0.04^\circ$  and  $0.05^\circ$ , corresponding to 823 kpc and 1080 kpc, for MS0353.6-3642 and MS0418.3-3844 respectively. The counts were corrected for the same King profile as previously and converted to fluxes and luminosities in an identical manner as before.

### 2.3 Surface brightness fitting and determination of $r_c$ .

Measurements of the core radii,  $r_c$ , were made for each cluster to allow a more accurate conversion from the detected count rate to the total count rate. This was carried out by fitting a King profile to the surface brightness taking into account blurring by the PSPC psf. The free parameters were the right-ascension and declination of the cluster centre, the core radius, and the normalisation. The index,  $\beta$  was frozen at  $\frac{2}{3}$  and it was assumed that the cluster was symmetric. The measured value of the core radius was then used to recompute the total flux.

## 3 RESULTS.

### 3.1 The new luminosities.

A summary of the results of the recalculated luminosities is shown in Table 1 and Table 2.

The total luminosities are on (error-weighted) average  $1.28 \pm 0.08$  times greater than those in Gioia & Luppino (1994) and  $1.16 \pm 0.02$  times greater than those in Nichol et al. (1997) with  $r_c = 250$  kpc. Using the measured values of  $r_c$  these values become  $1.22 \pm 0.07$  and  $1.13 \pm 0.03$  respectively. A figure more representative of the actual average increase in luminosity is found by excluding the clusters MS0353.6-3642 and MS0418.3-3844, for which the count rate was extracted over a small aperture (and hence open to larger errors in correcting for a King profile).

Excluding these clusters the error-weighted average ratios become  $1.23 \pm 0.08 \times \text{EMSS}$  and  $1.16 \pm 0.03 \times \text{Nichol}$  for  $r_c = 250$  kpc and  $1.18 \pm 0.08 \times \text{EMSS}$  and  $1.13 \pm 0.03 \times \text{Nichol}$  for measured  $r_c$ . This latter value of  $1.18 \times \text{EMSS}$  will be used to correct the luminosities of the EMSS clusters for which there were no PSPC data available. Throughout the rest of this paper all comparisons will be made using luminosities calculated using measured core radii.

Note that the ratio for MS1241.5+1710 is calculated using the luminosity scaled from that given in Gioia & Luppino (1994) according to the new redshift measurement.

Four clusters in the sample have been reanalysed following a similar aperture method by Jones et al. (1998). We find that our fluxes in this paper are an average factor of  $1.12 \pm 0.02$  times larger than those measured by Jones et al. (1998). Although the detailed analysis used here is an improvement over that used by Jones et al. (1998), since we include core radii measurements, this comparison gives an estimate of the absolute accuracy of our luminosities.

#### 3.1.1 Luminosity differences as a function of core radius.

An important point is that the ratio of *ROSAT* aperture luminosities to EMSS luminosities is a relatively strong function of measured core radii (see Fig. 3). The error-weighted average ratio for clusters with  $r_c < 250$  kpc,  $1.10 \pm 0.03$  (68% confidence error on the mean) is significantly lower than that for clusters with  $r_c > 250$  kpc,  $2.30 \pm 0.12$  (or  $1.08 \pm 0.03$  for  $r_c < 250$  kpc and  $2.16 \pm 0.15$  for  $r_c > 250$  kpc excluding MS0353.6-3642 and MS0418.3-3844). The correlation of  $L_{\text{ap}}/L_{\text{EMSS}}$  with  $r_c$  is significant at  $>99.9\%$  confidence (correlation coefficient of 0.85). This correlation contributes part

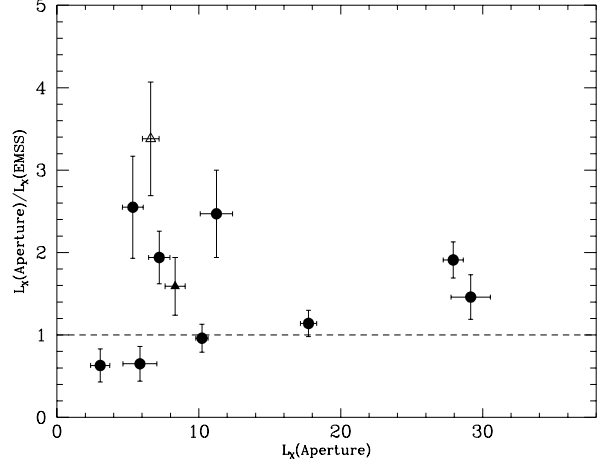


**Figure 1.**  $\frac{L_{\text{ap}}}{L_{\text{EMSS}}}$  as a function of  $L_{\text{ap}}$  (in units of  $10^{44}$  erg  $\text{s}^{-1}$ ). Circles denote that the counts were measured over a 3 Mpc radius, and triangles over a smaller radius. Open symbols denote that the temperature was assumed to be 6 keV, whilst closed symbols denote that the data have measured temperatures.

of the observed scatter on the mean luminosity ratio of all the clusters ( $1.18 \pm 0.08$ ).

The absolute broad-band flux calibration accuracy of the *ROSAT* PSPC ( $\approx 10\%$ ; Briel et al. 1996, *ROSAT* users handbook) and of the Einstein IPC (also  $\approx 10\%$ ; Harris & Irwin 1984, *EINSTEIN* revised user's manual) are smaller than the differences found, for example, in Fig 3, although they probably contribute part of the systematic difference observed. We note, however, that any calibration uncertainties cannot explain the observed correlation of  $\frac{L_{\text{ap}}}{L_{\text{EMSS}}}$  with core radius.

A key point made in this paper is that while the clusters with small core radii show reasonable agreement between *ROSAT* large aperture luminosities and EMSS luminosities, within the calibration uncertainties, the clusters with large core radii have significantly higher *ROSAT* luminosities.

### 3.2 Reasons for the luminosity differences.

To investigate possible causes for the differences between our results and those of the EMSS we show plots of  $\frac{L_{\text{ap}}}{L_{\text{EMSS}}}$  against  $L_{\text{ap}}$ ,  $z$  and  $r_c$  for clusters at  $z > 0.3$  in Fig. 1, Fig. 2 and Fig. 3. The errors in the ratios are calculated from counting statistics in the PSPC data combined with errors in the EMSS luminosities.

Figs. 1 and 2 show that there is no obvious trend of luminosity ratio with luminosity or redshift. Note that the highest point representing MS0418.3-3844 may be considered as misleading for reasons discussed above. The luminosity of the cluster MS0015.9+1609 given by the EMSS may be too low as it lies at the extreme edge of the IPC field (Henry 2000).

The reason for the difference in luminosity for clusters of high core radius may have its origins in the conversion of detected count rate to total flux. There are two stages in this conversion when an error could be introduced to the conversion factor. These are the conversion from detected

**Table 1.** A comparison of luminosities as measured by various authors. † means the count rate was extracted over a small aperture and ‡ means the temperature of the cluster was assumed to be 6 keV. \* The quoted EMSS luminosity for MS1241.5+1710 has been scaled from the Gioia & Luppino (1994) value according to the new redshift measurement.

Name	Redshift	EMSS	Luminosity $\times 10^{44}$ ergs s $^{-1}$		(0.3 – 3.5 keV)	
			Nichol	Ellis ( $r_c = 250$ kpc)	Ellis ( $r_c$ measured)	$r_c$ /kpc
MS0015.9+1609	0.546	14.64±1.63	22.78±0.54	27.96±0.71	27.93±0.71	247 $^{+5}_{-8}$
MS0353.6-3642†	0.320	5.24±1.06	8.70±0.73	8.65±0.74	8.33±0.71	225 $^{+37}_{-31}$
MS0418.3-3844†‡	0.350	1.433±0.264	1.49±0.096	4.84±0.33	6.61±0.43	474 $^{+92}_{-75}$
MS0451.6-0305	0.55	19.98±3.58	22.36±1.14	30.02±1.43	29.16±1.39	168 $^{+8}_{-7}$
MS0811.6+6301	0.312	2.10±0.42	1.99±0.5	5.30±0.73	5.35±0.73	280 $^{+77}_{-61}$
MS1241.5+1710	0.549	9.05* ± 2.31		6.05±1.23	5.85±1.19	204 $^{+30}_{-27}$
MS1358.4+6245	0.327	10.62±1.86	9.65±0.29	10.65±0.44	10.22±0.43	132 $^{+4}_{-5}$
MS1426.4+0158	0.320	3.71±0.48	5.38±0.46	7.08±0.78	7.21±0.75	302 $^{+43}_{-38}$
MS1512.4+3647	0.372	4.81±1.05	5.83±0.54	3.20±0.71	3.05±0.68	114 $^{+14}_{-14}$
MS1621.5+2640	0.426	4.55±0.856		10.35±1.05	11.28±1.14	480 $^{+95}_{-81}$
MS2137.3-2353	0.313	15.62±2.13	17.11±0.45	19.03±0.62	17.73±0.57	49 $^{+2}_{-3}$

**Table 2.** The ratios of luminosities measured here to previous measurements. The symbols † and ‡ are the same as in Table 1. The symbol ♣ refers to the averages when the clusters MS0418 and MS0353 are not included, for a correct comparison.

Name	Ratio ( $r_c = 250$ kpc)		Ratio ( $r_c$ measured)	
	EMSS	Nichol	EMSS	Nichol
MS0015.9+1609	1.91±0.22	1.23±0.04	1.91±0.22	1.23±0.04
MS0353.6-3642†	1.65±0.36	0.99±0.12	1.59±0.35	0.96±0.11
MS0418.3-3844†‡	2.61±0.53	2.51±0.28	3.38±0.69	3.25±0.36
MS0451.6-0305	1.50±0.29	1.34±0.09	1.46±0.27	1.30±0.09
MS0811.6+6301	2.52±0.61	2.66±0.76	2.55±0.62	2.69±0.77
MS1241.5+1710	0.67±0.22		0.65±0.21	
MS1358.4+6245	1.00±0.18	1.10±0.06	0.96±0.17	1.06±0.54
MS1426.4+0158	1.91±0.32	1.32±0.18	1.94±0.32	1.34±0.18
MS1512.4+3647	0.66±0.21	0.55±0.13	0.63±0.20	0.52±0.13
MS1621.5+2640	2.28±0.49		2.48±0.53	
MS2137.3-2353	1.22±0.17	1.11±0.05	1.14±0.16	1.04±0.04
Average	1.28±0.08	1.16±0.02	1.22±0.07	1.13±0.03
♣	1.23±0.08	1.16±0.03	1.18±0.08	1.13±0.03

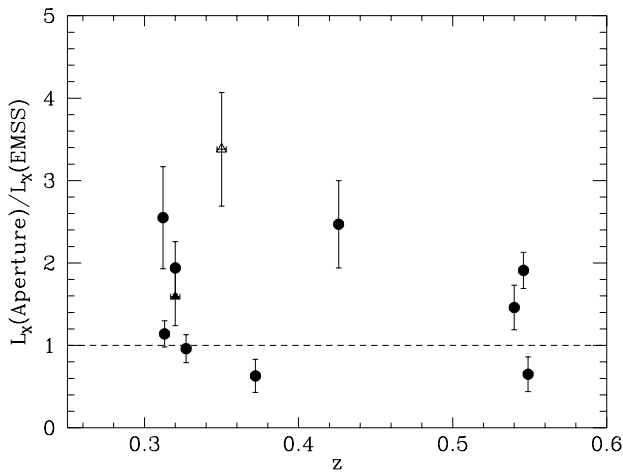


**Figure 2.**  $\frac{L_{\text{Ap}}}{L_{\text{EMSS}}}$  as a function of  $z$ . Symbols are the same as in Fig 1.

count rate to total count rate and the conversion from total count rate to flux.

The conversion from count rate to flux is dependent on

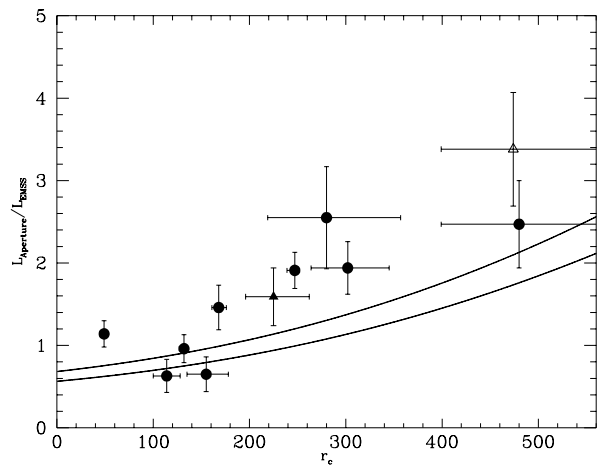


**Figure 3.**  $\frac{L_{\text{Ap}}}{L_{\text{EMSS}}}$  as a function of core radius (in units of  $h_{50}^{-1}$  kpc). Symbols are the same as in Fig 1. The lower line is the predicted ratio of the true luminosity to that assuming  $r_c = 250$  kpc; the upper line is the lower one multiplied by the correction for the IPC psf blurring (a factor of 1.21). See the discussion for details.

the spectral model used and the parameters specific to it. We have used a Raymond and Smith spectral model following Henry et al. (1992), but we have included previously unavailable measured values for the X-ray temperature,  $T_X$ . To examine the size of the effect that the value of  $T_X$  used in the spectral model has on the conversion factor the flux and luminosity of the coolest (MS1512.4+3647) and hottest (MS0451.6-0305) cluster were recalculated assuming  $kT = 6$  keV as in Henry et al. (1992). For MS1512.4+3647  $\frac{f(6\text{keV})}{f(3.57\text{keV})} = 1.12$  and  $\frac{L(6\text{keV})}{L(3.57\text{keV})} = 1.06$ , and for MS0451.6-0305  $\frac{f(6\text{keV})}{f(10.4\text{keV})} = 0.94$  and  $\frac{L(6\text{keV})}{L(10.4\text{keV})} = 1.00$ . Thus it can be seen that the conversion from count rate to flux is relatively insensitive to the exact value of temperature used in the spectral model and the discrepancy must have its origins in the conversion from detected to total count rate.

A possible source of error in the conversion from detected to total count rate is the assumed surface brightness profile used. This is especially important when converting from the detected count rate in the  $2.4' \times 2.4'$  detect cell of the EMSS to the total count rate as the correction is large. This correction is very sensitive to the model parameters used, especially the value used for the core radius. In Henry et al. (1992) it was assumed that  $r_c = 250$  kpc, whereas our surface brightness fitting gave measured values of  $r_c$  ranging from 49 kpc to 480 kpc (albeit with rather large errors on the larger clusters). It would be expected that for clusters whose actual core radius is less than 250 kpc the EMSS would *overestimate* the conversion from detected to total count rate. Conversely, clusters with  $r_c > 250$  kpc would be underestimated in the EMSS as there would be more emission lying outside the detect cell than accounted for assuming  $r_c = 250$  kpc.

Fig 3 shows that there is a trend where  $\frac{L_{\text{ap}}}{L_{\text{EMSS}}}$  increases with  $r_c$ , as expected. The underestimation becomes progressively bigger for larger clusters. The lower solid line in Fig. 3 gives the predicted luminosity ratio based on the constant  $r_c = 250$  kpc of Henry et al. (1992), i.e. the predicted ratio is unity for  $r_c = 250$  kpc. Most clusters lie above this line. Thus the EMSS assumption of a constant core radius cannot explain all of the observed discrepancy. There may be a further systematic difference between the luminosities.

### 3.3 The *EINSTEIN* IPC PSF.

Another source of possible error has been pointed out by Henry (2000); the conversion from detected flux to total flux in Henry et al. (1992) (equation 1 of that paper) does not include the effect of the IPC point spread function (psf). Furthermore Henry (2000) calculates that the effect of including the psf would be to increase the factor used to convert the number of counts in the detect cell to total counts,  $1/f$ , by 1.373 for clusters at  $0.3 < z < 0.6$ . This effect would explain the discrepancy we have measured.

The effect of the IPC psf was investigated further. Firstly it was checked whether the psf of the IPC is dependent on the off-axis angle of the source. Twenty four bright AGN in the EMSS survey (Gioia et al. 1990) were selected and a Gaussian profile was fitted to a radial plot of surface brightness in the EMSS detection energy band of 0.2 – 3.5 keV. It was found that the full width at half maximum of the Gaussian did not show any trends with

off-axis angle. The reason for this lack of trend is that the electronics of the IPC dominate the scattering from the mirrors (Giacconi et al. 1979). Having established that the psf of the IPC+mirror combination is independent of off-axis angle, the on-axis psf was used to investigate what effect this would have on the fraction of measured flux to total flux. A pure Gaussian is used to model the IPC psf since the flux lost into the non-Gaussian wings of the combined IPC+mirror psf, at large radii, caused by mirror scattering, has already been accounted for in the EMSS fluxes. The psf used was taken from the average measurement of the AGN Gaussian profiles and had  $\text{FWHM} = 92'' \pm 5''$ .

For each cluster a model King profile was constructed from the measured values of core radii and an assumed value of  $\beta = \frac{2}{3}$ . This was then blurred by convolving it with the IPC psf. From this dataset the ratio of counts,  $f_{\text{psf}}$ , falling within a  $2.4' \times 2.4'$  square centred on the cluster and a circle of radius  $30'$  (approximately the total counts) was measured. This was compared to the predicted ratio between the same two apertures assuming a pure King profile without blurring,  $f_{\text{King}}$ , as used in Henry et al. (1992).

For the eleven clusters remeasured in this work the assumption of a pure King profile gives total counts that are on average a factor of 0.83 too small, i.e. the original EMSS fluxes need increasing by a factor of 1.21. This is slightly lower than, but still comparable to, the result obtained in Henry (2000) of an increase of 1.373 in converting from counts in a  $2.4' \times 2.4'$  cell to total counts. The difference in the two results is due mainly to the size of the psf used in calculating  $f_{\text{psf}}$  (Henry 2000 uses  $\text{FWHM} = 105''$ , private communication) and partly due to the inclusion of measured core radii of individual clusters. As a check we calculated  $f_{\text{psf}}$  for an assumed 250 kpc cluster in the redshift range  $z = 0.3$ – $0.6$  and find values of  $\frac{f_{\text{King}}}{f_{\text{psf}}}$  of 1.28 and 1.34 for psfs of  $92''$  and  $105''$  respectively. We have elected to use the value of  $\text{FWHM} = 92''$  as measured from IPC data (we note that the  $\text{FWHM}$  for clusters, with harder IPC spectra than AGN, may be anything less than  $92''$ ).

The redshift dependence of the effect of the psf on the conversion from detected to total counts is shown in figure 4. This was calculated for an on-axis cluster of  $r_c = 250$  kpc. It can be seen that between  $z = 0.15$  and  $z = 0.6$  there is almost no change in  $\frac{f_{\text{psf}}}{f_{\text{King}}}$ ; this is because the psf is larger than the cluster at such high redshifts.

### 3.4 The new X-Ray luminosity function.

Using the new luminosities discussed above the X-ray luminosity function was computed and compared to the EMSS XLF computed using the data from Gioia & Luppino (1994). In the sample of Gioia & Luppino (1994) there are 24 clusters with  $z > 0.3$  and measured luminosities. In our sample taken from Gioia & Luppino (1994) there are only 21 clusters having these criteria. It is only these 21 clusters which are used in computing the luminosity functions. (The reasons for the differences between the samples are that MS1333.3+1725 has now been identified as a star (Luppino et al. 1999), MS1209.0+3917 as a BL Lac (Rector et al. 1998) and MS1610.4+6616 as a point source at the position of a star (Stocke et al. 1999). Note that MS0354.6-3650 which appears in Henry et al. (1992) does not appear in Gioia

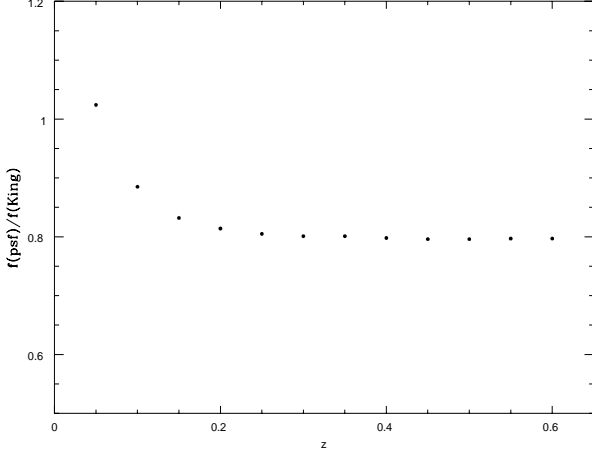


**Figure 4.**  $\frac{f_{\text{psf}}}{f_{\text{King}}}$  as a function of redshift.

& Luppino (1994) and appears to be a soft X-ray source (Nichol et al. 1997).

The XLF was computed using the  $\frac{1}{V_a}$  method of Avni & Bahcall (1980) as used in the non-parametric analysis of Henry et al. (1992). This method is summarised here.

For each cluster the luminosity distance and the angular size of the core radius (as measured) were calculated according to the formulae below,

$$D_L = \frac{c}{q_0^2 H_0} (q_0 z + (q_0 - 1)(\sqrt{1 + 2q_0 z} - 1)) \quad (1)$$

$$\theta_0 = \frac{r_c(1+z)^2}{D_L} \quad (2)$$

The fraction of counts which fell inside the detect cell of  $2.4' \times 2.4'$  was calculated according to,

$$f = \frac{2}{\pi} \arcsin \left\{ \frac{\left(\frac{\theta_D}{\theta_0}\right)^2}{\left(\left(\frac{\theta_D}{\theta_0}\right)^2 + 1\right)} \right\} (g_{\text{psf}}) \quad (3)$$

where  $\theta_D$  is the angular half size of the detect cell and  $g_{\text{psf}} = \frac{f_{\text{psf}}}{f_{\text{King}}}$  is a new factor which takes into account the effect of the IPC psf. As fig 4 shows, the effect of the IPC psf is constant for a particular cluster above  $z = 0.3$ , so the inclusion of  $g_{\text{psf}}$  is unimportant here as it will cancel out in equation 4 below.

The maximum redshift at which the cluster could have been detected was calculated for each flux limited observation making up the survey. This was found by incrementing  $z_{\text{max}}$  in the following formula until the statistic, *FIT* gave the value closest to 1, where

$$FIT = \frac{F_{\text{DET}}}{F_{\text{LIM}}} \left( \frac{D_L(z)}{D_L(z_{\text{max}})} \right)^2 \left( \frac{f(z_{\text{max}})}{f(z)} \right) \quad (4)$$

where  $F_{\text{DET}}$  is the detect cell flux at the observed redshift  $z_{\text{obs}}$ , and  $F_{\text{LIM}}$  is the limiting survey flux.

The total volume in which each cluster could have been found was then calculated by summing over all the flux limits

$$V_a = \sum_i \left[ \frac{dV(\Omega_0, \leq \min(z_u, z_{\text{max},i})}{d\Omega} \right]$$

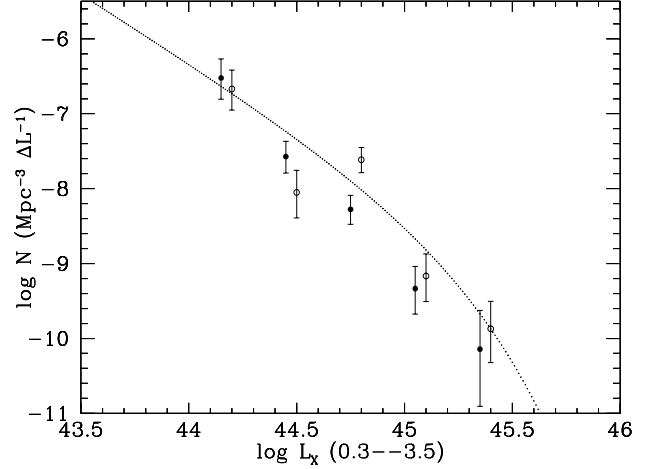


**Figure 5.** The revised X-ray Luminosity Function at  $z = 0.3 - 0.6$ . Closed circles are from the data of Gioia & Luppino (1994) and open circles are from PSPC data. The dotted line is the local BCS XLF from Ebeling et al. (1997).

$$- \left. \frac{dV(\Omega_0, \leq z_i)}{d\Omega} \right] d\Omega_{\text{surv},i} \quad (5)$$

where  $z_u$  and  $z_l$  are the upper and lower redshift limits of the sample and  $d\Omega_{\text{surv},i}$  is the solid angle associated with the  $i$ th flux limit. The mean ratio of the search volumes found here to those assuming no blurring from the IPC psf and a constant core radius of  $r_c = 250\text{kpc}$  (as in Henry et al. (1992)) was  $0.99 \pm 0.03$ .

The values for  $\frac{dV}{d\Omega}$  were calculated by numerical integration of the following equation

$$\frac{dV}{d\Omega dz} = 4 \left( \frac{c}{H_0} \right)^3 \frac{[\Omega_0 z + (2 - \Omega_0)(1 - \sqrt{1 + \Omega_0 z})]^2}{\Omega_0^4 (1+z)^3 \sqrt{1 + \Omega_0 z}} \quad (6)$$

with respect to  $z$ .

The clusters were binned up into log luminosity bins that are 0.3 wide and then the differential luminosity function was calculated for each bin

$$n(L) = \sum_{j=1}^n \frac{1}{V_{a,j} \Delta L} \quad (7)$$

where  $\Delta L$  is the width of the luminosity bin and  $n$  is the number of clusters in that bin.

The XLF is recomputed using the remaining 21 clusters from Gioia & Luppino (1994) and compared to our XLF in two ways. Firstly using our new luminosities for those clusters observed by the PSPC and the luminosities of Gioia & Luppino (1994) for those clusters not observed by the PSPC. This is shown in Fig. 5. Secondly the luminosities of the clusters not observed by the PSPC are corrected by the average increase measured (when not including MS0418.3-3844 and MS0353.6-3642). This is shown in Fig. 6.

Superimposed on both Fig. 5 and Fig. 6 is the best fitting Schechter function to the local XLF from Ebeling et al. (1997) which is obtained from the *ROSAT* Brightest Cluster Sample (BCS). All the luminosities we have used to calculate the XLFs in Figs. 5 and 6 are based on an integration of the emission to infinity, as is the BCS XLF. In Fig. 7 we compare the updated XLF with the local XLF of Böhringer

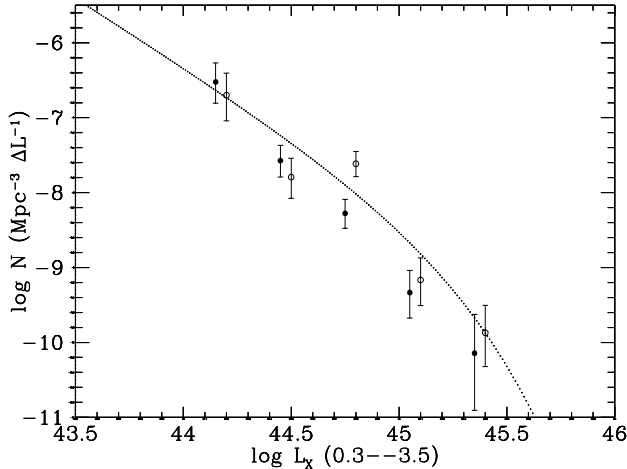


**Figure 6.** The revised X-ray Luminosity Function at  $z = 0.3 - 0.6$ . Symbols are the same as in Fig. 5 except that clusters for which there are no PSPC data have had their luminosities corrected by the average correction factor of 1.18.

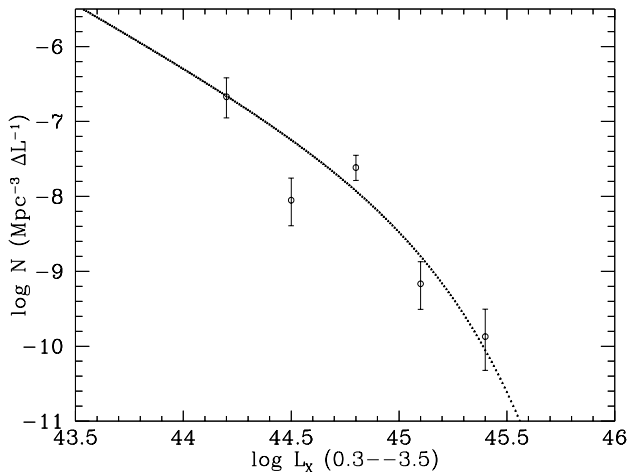


**Figure 7.** The revised X-ray Luminosity Function at  $z = 0.3 - 0.6$ , compared to the local XLF of Böhringer et al. (2001). The data points are based on the revised luminosities, including an average correction factor for clusters with no PSPC data, but all luminosities have then been decreased by 8%, to be consistent with the approximation used by Böhringer et al. for integrating only to the virial radius.

et al. (2001), which updates the work of De Grandi et al. (1999) and which was published while this paper was being produced. The Böhringer et al. XLF was also converted from the 0.1–2.4 keV band to the 0.3–3.5 keV band. For cluster temperatures of  $T_X = 4-10$  keV, a conversion factor of  $L_{0.3-3.5} = 1.1L_{0.1-2.4}$  is accurate to within  $\approx 8\%$ . Böhringer et al. use luminosities measured by integrating to the virial radius, approximated by 12 times the core radius. As noted by Böhringer et al. (2000), this approximation gives a systematic decrease of 8% compared to integrating to infinity. The same data as in Fig. 6 are plotted, except that all the luminosities were reduced by 8%, to be consistent with the virial radius approximation used by Böhringer et al..

It is clear that whereas previously there existed evidence for a degree of evolution from the local XLF the effect of the increase in luminosity is to bring the high redshift XLF back in line with it. This appears to be the case in Figs. 5, 6 and 7.

### 3.5 Tests of evolution.

An alternative test for the presence of evolution is to compare the observed number of clusters at  $0.3 < z < 0.6$  to the number predicted based on a non-evolving local XLF and the sky coverage of the survey.

Two local XLFs were used in this test, that of Ebeling et al. (1997) and that of Böhringer et al. (2001). The local XLF was integrated over redshift ( $0.3 < z < 0.6$ ) and over luminosity ( $10^{43} - 10^{46}$  erg s $^{-1}$ ), to predict the number of clusters as a function of total flux. K-corrections were included for the 0.3–3.5 keV band based on temperatures estimated from the  $L_X-T$  relation of White et al. (1997), and calculated from *MEKAL* model spectra. The total fluxes were then converted to detect-cell fluxes using a single value of  $f$ , and the EMSS sky coverage of Henry et al. (1992) (which is defined as a function of detect-cell flux) used to give the total number of clusters predicted in the EMSS.

For the local XLF of Ebeling et al. (1997), the published 0.3–3.5 keV XLF could be used directly. Ebeling et al. (1997) used luminosities calculated by integrating the surface brightness to infinite radius, so the appropriate values of  $f$  to use were  $f_{\text{psf}} = 0.488 \pm 0.05$ , the mean value of the 11 clusters studied here including the effect of their measured core radii, and  $f_{\text{psf}} = 0.445$ , the value for a cluster with  $r_c = 250$  kpc at  $z=0.387$  (the mean redshift of the EMSS  $0.3 < z < 0.6$  sample). For comparison,  $f_{\text{King}} = 0.593 \pm 0.06$ , again the mean over the 11 clusters, was also used. Using  $f_{\text{King}}$  neglected the effect of the *EINSTEIN* IPC psf.

The local XLF of Böhringer et al. (2001) has a different normalisation definition to that of Ebeling et al. (1997), and was also converted from the 0.1–2.4 keV band to the 0.3–3.5 keV band as above. Böhringer et al. only integrate the emission to the virial radius. The approximation to the virial radius used by Böhringer et al. gives an decrease of 8% compared to integrating to infinity, independently of the value of the core radius. Thus the values of  $f$  we use are the values of  $f_{\text{psf}}$  as used for the Ebeling et al. (1997) XLF, but multiplied by 1.08.

The results are shown in Table 3. The number of clusters predicted ( $N_{\text{pred}}$ ) assuming no evolution of the XLF is given in the third column. In all cases this is more than the number observed ( $N_{\text{obs}} = 21 \pm 4.6$ ). The mean of the two best no-evolution predictions is 42, twice the number observed. The significance of the difference, in units of sigma, is given in the following column. Errors on the predicted numbers were derived from the square root of the total number of clusters in each of the local surveys.

## 4 DISCUSSION.

### 4.1 The new luminosities.

The ratio of the luminosities of clusters with  $z > 0.3$  as measured by our aperture photometry using *ROSAT* PSPC data



**Table 3.** Results of the tests of the evolution of the XLF.

Local XLF	$f$	$\frac{1}{f}$	$N_{\text{pred}}$	Significance of $N_{\text{pred}} - N_{\text{obs}}^b$ ( $\sigma$ )	Notes on $f^a$
BCS <sup>c</sup>	0.488	2.05	$35.9 \pm 2.5$	2.8	$\overline{f_{\text{psf}}}$ ; mean over 11 clusters
BCS	0.445	2.25	$31.3 \pm 2.2$	2.0	$f_{\text{psf}}$ for $r_c = 250$ kpc, $z = 0.39$
(BCS	0.593	1.69	$47.9 \pm 3.4$	4.7) <sup>d</sup>	$\overline{f_{\text{King}}}$ ; mean over 11 clusters
REFLEX <sup>e</sup>	0.527	1.90	$46.4 \pm 2.2$	4.9	$\overline{f_{\text{psf}}} \times 1.08$ to account for the REFLEX luminosities within $12r_c$
REFLEX	0.489	2.08	$40.3 \pm 1.9$	3.9	$f_{\text{psf}} \times 1.08$ ; for $r_c = 250$ kpc, $z = 0.39$
REFLEX	0.427	2.34	$33.1 \pm 1.6$	2.5	$f_{\text{psf}} \times 1.08$ ; for $r_c = 300$ kpc, $z = 0.39$
REFLEX	0.545	1.83	$49.0 \pm 2.3$	5.5	$\overline{f_{\text{psf}}} \times 1.08$ ; for $r_c = 200$ kpc, $z = 0.39$
(REFLEX	0.640	1.56	$62.5 \pm 2.9$	7.6) <sup>d</sup>	$\overline{f_{\text{King}}} \times 1.08$

<sup>a</sup> See text for full explanation

<sup>b</sup>  $N_{\text{obs}} = 21 \pm 4.6$

<sup>c</sup> BCS XLF of Ebeling et al. (1997)

<sup>d</sup> Use of  $f_{\text{King}}$  rather than  $f_{\text{psf}}$  is incorrect but is included to show the sensitivity of  $N_{\text{pred}}$  on  $f$ .

<sup>e</sup> REFLEX XLF of Böhringer et al. (2001)

and as measured in the original EMSS has been investigated. The ratio is found to be correlated with the core radius of the cluster. For clusters with small core radii the *ROSAT* and EMSS luminosities are in agreement, within the instrumental calibration uncertainties. For clusters with progressively larger core radii, the *ROSAT* luminosities increase to  $\approx 2$  times the EMSS luminosities. A straightforward explanation of the correlation is that for larger clusters ( $r_c > 250$  kpc) more flux would fall outside the detect cell than predicted by Henry et al. (1992), who assumed a constant 250kpc core radius.

An additional difference is probably caused by the omission of the *Einstein* IPC point spread function when converting from detected flux to total flux, as suggested by Henry (2000). We have shown that the inclusion of the psf would increase the EMSS fluxes by a factor  $\approx 1.21$  for clusters at  $z > 0.3$ . The combination of this factor together with the measured core radii can account for most of the observed difference in luminosity as shown in Fig 3. The lower line in Fig 3 shows the predicted ratio of true luminosity to the luminosity derived from an EMSS detect cell flux, assuming a fixed core radius of 250kpc (at a redshift of  $z = 0.4$ ). The upper line shows the effect of including IPC psf blurring in this prediction. For clusters with small core radii ( $< 250$  kpc), the overestimate of EMSS luminosity due to the assumption of a fixed core radius may in part have been cancelled by the underestimate due to the effect of the *Einstein* IPC psf. For clusters with large core radii ( $> 250$  kpc), however, the two effects work in the same direction, which would produce an underestimated EMSS luminosity.

#### 4.1.1 Integrating to the virial radius.

In order to make comparisons with previous work, the luminosities discussed so far have been derived using the same method as in those works, ie. an extrapolation of a King profile to infinite radius (except when comparing with the XLF of Böhringer et al. 2001). If instead we define the luminosity  $L_{\text{vir}}$ , perhaps more accurately, as that within a King

profile truncated at the virial radius  $r_{\text{vir}}$  (as suggested by Henry 2000), where  $r_{\text{vir}} \approx 1.8$  Mpc for a  $T = 6$  keV cluster at  $z = 0.4$ , then the luminosities we calculate would decrease. The size of the decrease depends on the core radius and the temperature, but would typically be  $\approx 13\%$  for a  $T = 6$  keV,  $r_c = 250$  kpc cluster, and 3%–25% for  $r_c = 50$ –500 kpc. Thus, as noted by Henry (2000), the original EMSS  $z > 0.3$  luminosities fortuitously give approximately accurate mean values of  $L_{\text{vir}}$ , since the 13% decrease in the *ROSAT* luminosities would nearly cancel the average 18% difference between the *ROSAT* and EMSS luminosities.

What would  $L_{\text{vir}}$  be for clusters with different core radii? Using  $r_{\text{vir}} = r_{200} = 3.89(T_x/10\text{keV})^{1/2}(1+z)^{-3/2}$  Mpc (for  $H_0=50$ ; Evrard et al. 1996),  $r_{\text{vir}} = 1.84$  Mpc for a  $T_x = 6$  keV cluster at  $z = 0.39$ , the mean redshift of the 21 clusters in the EMSS sample. For a core radius of 150 kpc, the *ROSAT* values of  $L_{\text{vir}}$  would be 8% lower than the luminosities quoted in Tables 1 and 2. The ratio of *ROSAT* to EMSS luminosities for clusters with  $r_c < 250$  kpc would then be in even better agreement, with a mean ratio of  $1.0 \pm 0.3$ .

For a core radius of 350 kpc, the *ROSAT* values of  $L_{\text{vir}}$  would be 19% lower than the luminosities quoted in Tables 1 and 2. The ratio of *ROSAT* to EMSS luminosities for clusters with  $r_c > 250$  kpc would then be  $1.81 \pm 0.15$ , still significantly larger than unity.

Summarizing, for small ( $r_c < 250$  kpc) clusters there is good agreement between the *ROSAT* and EMSS luminosities, especially if the *ROSAT* luminosities are derived from an integration only within the virial radius. For large clusters ( $r_c > 250$  kpc), the agreement is less good, and here we suspect that the EMSS luminosities need increasing by a factor of 1.8–2.2, depending on the radial integration limit used. How many clusters have large core radii? In the local sample of Vikhlinin et al. (1999) half of all clusters (19 of 39) have  $r_c > 250$  kpc (consistent with the 4 out of the 11 clusters studied here), and a third have  $r_c > 300$  kpc. Thus a substantial fraction of the cluster population is affected.

#### 4.1.2 *ASCA luminosities.*

It is also noted in Henry (2000) that there is a discrepancy between *ASCA* fluxes and EMSS fluxes with *ASCA* fluxes being a factor 1.17 higher (or 1.12 excluding MS0015.9+1609), a figure very consistent with the value  $1.18 \pm 0.08$  found in this paper. It is suggested in Henry (2000) that the reason here is the contamination of the measured flux by unrelated sources in the GIS extraction beam. This explanation is in conflict with the previous explanation of the *ROSAT*/EMSS discrepancy. The *ROSAT*/EMSS discrepancy is explained if the EMSS fluxes are *increased* by 1.21 (the effect of including the IPC psf), whereas the *ASCA*/EMSS discrepancy is explained if the *ASCA* fluxes are *decreased* to bring them into line with the EMSS fluxes (because of unrelated sources in the *ASCA* beam). Clearly both of the explanations cannot be true.

## 4.2 Evolution of the cluster space density.

We have made two tests of the degree of evolution based on the EMSS cluster luminosities at  $0.3 < z < 0.6$ .

The comparison of the number of observed clusters with that predicted from an integration of the local XLF over redshift and luminosity, assuming no evolution, has some advantages. It includes the effect of non-detections, and does not use the luminosities directly, only the total number of clusters above the flux limits of the survey. A disadvantage is that, for the EMSS, a correction has to be made from the total flux predicted (based on the integration of the local XLF), to a detect cell flux. Without accurate knowledge of the distribution of surface brightness shapes at high redshift (eg. core radii), a mean value of the core radius has to be used for this correction.

The results of the comparison are that for the BCS XLF of Ebeling et al. (1997), the observed number of clusters is a factor of 1.7 lower than the no-evolution prediction, at a significance of  $2.8\sigma$ . For the REFLEX XLF of Böhringer et al. (2001), the observed number of clusters is a factor of 2.2 lower than the no-evolution prediction, at a significance of  $4.9\sigma$ . These predictions are sensitive to the mean value of  $f$  assumed; for values of  $f$  corresponding to mean core radii of 200 kpc – 300 kpc, the significance of the difference from no-evolution varies from  $5.5\sigma$  to  $2.5\sigma$ .

The second test was the updated binned EMSS XLF. The XLF has the advantage of an individual correction to total flux for each cluster (at least for those with measured core radii), but has the disadvantages of excluding luminosities where no clusters were detected, and the somewhat arbitrary choice of binning. The updated XLF is consistent with no evolution, and, given the size of the error bars on the binned XLF, consistent with a factor of  $\approx 2$  decrease in the normalisation of the XLF at  $z \approx 0.4$  suggested by the first test.

When predicting the number of clusters from the local XLFs, we have used Schechter function parameterizations of the local XLFs. These are good fits for most luminosities. However, at the highest luminosities ( $L_X > 10^{45}$  erg s $^{-1}$ , 0.1–2.4 keV) Figs. 1 and 4 of Böhringer et al. (2001) show that the Schechter function fit overestimates the number of clusters in the REFLEX XLF by a factor  $\approx 1.7$  which increases with luminosity (the Schechter function fit underestimates

the number of clusters at lower luminosities  $L_X \approx 10^{44}$  erg s $^{-1}$ , but by a smaller factor  $\approx 1.3$ ). The cause of the overestimate at high luminosities may be small number statistics or real deviations from a Schechter function. In either case, if the number of high luminosity clusters observed in the REFLEX survey were used, rather than the Schechter function fit, the effect would be to reduce the no-evolution prediction. Approximately 25% of the EMSS sample have  $L_X > 10^{45}$  erg s $^{-1}$ , and  $\approx 15\%$  have  $L_X < 2 \times 10^{44}$  erg s $^{-1}$ , so this would be a relatively small net effect, reducing the predictions in Table 3 by  $\approx 10\%$ , and therefore reducing the  $4.9\sigma$  significance to  $4.2\sigma$ . The significance would be reduced slightly further if we based the errors in the predicted numbers on only the number of clusters in the local XLFs that have luminosities which match those in the  $0.3 < z < 0.6$  EMSS sample ie  $L_X > 10^{44}$  erg s $^{-1}$ , rather than the full number in the local XLF.

Another uncertainty arises from the suggestion of Ebeling et al. (2000) that the EMSS may be incomplete due to a systematic bias against unrelaxed clusters. Ebeling et al. suggest that the bias may be more pronounced for high luminosity clusters at intermediate to high redshift, providing an alternative explanation for some of the negative evolution observed in the EMSS.

In summary, based on one of two local XLFs, we find that the predicted number of clusters may be inconsistent with no evolution (but with caveats), whilst using another local XLF (but containing a smaller number of clusters) gives a less significant result. Both no-evolution predictions are a factor of  $\approx 2$  higher than the observed number of clusters, although the predictions are sensitive to  $f$ , the correction from total to detect cell fluxes, and we have used a mean value of  $f$ . The binned XLF is consistent with no evolution, but also with a factor of  $\approx 2$  evolution in the number of clusters. Overall, we conclude that the space density of  $0.3 < z < 0.6$  EMSS clusters, based on their updated luminosities, is consistent with either no evolution or a factor of  $\approx 2$  fewer clusters.

A factor of two evolution in the cluster space density is consistent with that found by Henry et al. (1992) at  $L_X = 3 \times 10^{44}$  erg s $^{-1}$ , but we do not find larger evolutionary factors at higher luminosities, as suggested by an extrapolation of the power law XLF fits of Henry et al. (1992). At the highest luminosities sampled,  $L_X = 1 \times 10^{45} - 3 \times 10^{45}$  erg s $^{-1}$  (0.3–3.5 keV), there are  $5^{+3.4}_{-2.2}$  clusters in the updated sample, compared with 9.1 predicted from a non-evolving REFLEX XLF (using  $f_{psf}=0.527$ ), and 9.0 predicted from the BCS XLF (using  $f_{psf}=0.488$ ). Evolution by a large factor of 9 in the XLF normalisation, for example, giving a prediction of one cluster at these luminosities, is ruled out at  $>99\%$  confidence by the 5 observed.

The little or no evolution of the XLF observed in this work has important consequences for future and past work that concern cluster evolution based on the EMSS sample. As was stressed in the introduction the EMSS is very suited to constraining cluster evolution due to the (relatively) high number of high luminosity, massive clusters at high redshift which it contains.

One measurement which can be made using the constraint of little or no evolution of the XLF is to constrain the matter density parameter of the Universe,  $\Omega_0$ . Little or no evolution favours a low  $\Omega_0$  universe (Kay & Bower 1999).

This result is in contrast with that of previous determinations of  $\Omega_0$  based on the apparent evolution in the EMSS XLF. Reichart et al. (1999) find  $\Omega_0 = 0.96$  from their analysis of the evolution of the high redshift sample of EMSS XLF compared to the BCS. Sadat et al. (1998) also derive a high value of  $\Omega_0$  ( $= 0.85 \pm 0.2$ ) from their work on the  $L_X$ - $T_X$  relation and the redshift distribution of the EMSS sample which is supported by the work of Blanchard & Bartlett (1998).

### 4.3 Search volumes and consequences for the X-ray temperature function.

The revised luminosities of clusters in the EMSS could also have an effect on other studies based on the EMSS sample. The new core radii not only change the values of the luminosity used in calculating the XLF but they also slightly alter the search volumes used. Because the new volumes are not systematically larger or smaller than search volumes calculated assuming  $r_c = 250$  kpc and no blurring due to the IPC psf they only have a small effect on the XLF. The neglect of the IPC psf blurring has almost no effect on the calculated volumes, because  $g_{\text{psf}}$  cancels out in equation 4 and  $g_{\text{psf}}$  is essentially independent of redshift at  $z > 0.3$ .

Henry (2000) and Donahue et al. (1999) use temperatures measured from *ASCA* for the EMSS high- $z$  sample to determine the evolution of the temperature function, and derive important measurements of  $\Omega_0$ . Search volumes are determined in a similar way as described above, from values of  $f$  as a function of redshift, and detect cell fluxes. We find that the search volumes are affected little by the assumption of a core radius of 250 kpc compared to using the measured core radii (the difference for the clusters with  $r_c > 250$  kpc is  $\leq 3\%$ ), or by neglecting the IPC psf blurring (since the effect of  $g_{\text{psf}}$  cancels out).

## 5 CONCLUSIONS.

The X-ray luminosities of 11 EMSS clusters at  $0.3 < z < 0.6$  have been remeasured using *ROSAT* PSPC data, including a measurement of the core radii, and using large apertures to avoid uncertain extrapolations of the surface brightness. For clusters with core radii  $r_c < 250$  kpc, we find reasonable agreement between the *ROSAT* luminosities and the original luminosities of Henry et al. (1992) and Gioia & Lupino (1994) (a mean ratio of  $1.08 \pm 0.03$ ). For clusters with large core radii,  $r_c > 250$  kpc, the *ROSAT* luminosities are  $2.2 \pm 0.15$  times the EMSS luminosities. This difference can be largely explained by the assumption of a fixed core radius (of 250 kpc) in the EMSS, combined with the omission of the effect of the *EINSTEIN* IPC psf in calculating the total fluxes. These effects are most important in deriving accurate luminosities. The effect on the EMSS cluster survey search volumes, which are used in both luminosity function and temperature function studies, is small.

The binned EMSS XLF at  $0.3 < z < 0.6$ , based on the new luminosities and on an updated sample, is consistent with no evolution. The predicted numbers of clusters, assuming no evolution and based on two local luminosity functions, is  $\approx 2$  times the number observed at  $0.3 < z < 0.6$ . Given the uncertainties in the luminosities, in the derivation of detect cell

fluxes, and the relatively small numbers of luminous clusters in both the EMSS and in the local samples, we conclude that the updated EMSS sample is consistent with either no evolution of the space density of luminous clusters, or a small factor of  $\approx 2$  fewer luminous clusters at  $z=0.4$  (the mean redshift of the sample). Little or no evolution in the space density of luminous clusters is consistent with low values of  $\Omega_0$ .

## 6 ACKNOWLEDGMENTS.

The authors would like to thank Pat Henry for useful discussions. SCE acknowledges a PPARC studentship; LRJ also acknowledges PPARC support. This research has made use of data obtained from the Leicester Database and Archive Service at the Department of Physics and Astronomy, Leicester University, UK and the Einline service at the Harvard-Smithsonian Center for Astrophysics. The authors would also like to thank the referee for some important improvements.

## REFERENCES

- Allan D. J., Vallance R. J., 1995, Starlink User Note, 98.6
- Avni Y., Bahcall J. N., 1980, ApJ, 235, 694
- Blanchard A., Bartlett J. G., 1998, A&A, 332, L49
- Böhringer H. et al., 2000, ApJS, 129, 435
- Böhringer H. et al., 2001, astro-ph/0106243
- Briel U. G. et al., 1996, *ROSAT User's Handbook*. Max-Planck Institut für Extraterrestrische Physik (MPE)
- Burke D. J., Collins C. A., Sharples R. M., Romer A. K., Holden B. P., Nichol R. C., 1997, ApJ, 488, L83
- Cash W., 1979, ApJ, 228, 939
- De Grandi S. et al., 1999, ApJ, 513, L17
- Dickey J. M., Lockman F. J., 1990, ARA&A, 28, 215
- Donahue M., Voit G. M., Scharf C. A., Gioia I. M., Mullis C. R., Hughes J. P., Stocke J. T., 1999, ApJ, 527, 525
- Ebeling H., Edge A. C., Fabian A. C., Allen S. W., Crawford C. S., Böhringer H., 1997, ApJ, 479, L101
- Ebeling H. et al., 2000, ApJ, 534, 133
- Ebeling H., Jones L. R., Fairley B. W., Perlman E., Scharf C., Horner D., 2001, ApJ, 548, L23
- Evrard A. E., Metzler C. A., Navarro J. F., 1996, ApJ, 469, 494
- Giacconi R. et al., 1979, ApJ, 230, 540
- Gioia I. M., Lupino G. A., 1994, ApJS, 94, 583

- Gioia I. M., Henry J. P., Maccacaro T., Morris S. L., Stocke J. T., Wolter A., 1990, *ApJ*, 356, L35
- Gioia I. M., Henry J. P., Mullis C. R., 2001, *astro-ph/0102332*
- Harris D. E., Irwin D., 1984, *EINSTEIN Observatory Revised User's Manual*. Harvard-Smithsonian Center for Astrophysics
- Henry J. P., Gioia I. M., Maccacaro T., Morris S. L., Stocke J. T., 1992, *ApJ*, 386, 408
- Henry J. P., 2000, *ApJ*, 534, 565
- Jones L. R., Scharf C., Ebeling H., Perlman E., Wegner G., Malkan M., Horner D., 1998, *ApJ*, 495, 100
- Jones L. R. et al., 2000, in *Constructing the Universe with Clusters of Galaxies*, IAP 2000 meeting, Paris, eds Florence Durret & Daniel Gerbal
- Kay S. T., Bower R. G., 1999, *MNRAS*, 308, 664
- Luppino G. A., Gioia I. M., Hammer F., Le Fèvre O., Annis J. A., 1999, *A&AS*, 136, 117
- Molikawa K., Hattori M., Kneib J., Yamashita K., 1999, *A&A*, 351, 413
- Nichol R. C., Holden B. P., Romer A. K., Ulmer M. P., Burke D. J., Collins C. A., 1997, *ApJ*, 481, 644
- Nichol R. C. et al., 1999, *ApJ*, 521, L21
- Raymond J. C., Smith B. W., 1977, *ApJS*, 35, 419
- Rector T. A., Stocke J. T., Perlman E. S., 1998, *ApJ*, 516, 145
- Reichart D. E., Nichol R. C., Castander F. J., Burke D. J., Romer A. K., Holden B. P., Collins C. A., Ulmer M. P., 1999, *ApJ*, 518, 521
- Rosati P., Borgani S., Della Ceca R., Stanford A., Eisenhardt P., Lidman C., 2000, in *Large-Scale Structure in the X-ray Universe*, eds Plionis & Kolokotronis, Atlantisciences, p13
- Sadat R., Blanchard A., Oukbir J., 1998, *A&A*, 329, 21
- Snowden S. L., Plucinsky P. P., Briel U., Hasinger G., Pfeffermann E., 1992, *ApJ*, 393, 819
- Stocke J. T., Perlman E. S., Gioia I. M., Harvenek M., 1999, *AJ*, 117, 1967
- Vikhlinin A., McNamara B. R., Forman W., Jones C., Quintana H., Hornstrup A., 1998a, *ApJ*, 498, L21
- Vikhlinin A., McNamara B. R., Forman W., Jones C., Quintana H., Hornstrup A., 1998b, *ApJ*, 502, 558
- Vikhlinin A., Forman W., Jones C., 1999, *ApJ*, 525, 47
- White D. A., Jones C., Forman W., 1997, *MNRAS*, 292, 419